AGU PUBLICATIONS

Geophysical Research Letters

RESEARCH LETTER
10.1002/2016GL072247

**Key Points:**
- Tropospheric eddy heat fluxes by different zonal wave numbers are negatively correlated at low frequency
- This anticorrelation is key for the low-frequency suppression of the heat flux spectrum and associated oscillatory heat flux variability
- Low-frequency baroclinicity variability is driven by the mean meridional circulation and not suppressed

**Supporting Information:**
- Supporting Information S1

**Correspondence to:**
P. Zurita-Gotor,
pzurita@alum.mit.edu

**Citation:**
Zurita-Gotor, P. (2017), Low-frequency suppression of Southern Hemisphere tropospheric eddy heat flux, *Geophys. Res. Lett.*, *44*, 2007–2015, doi:10.1002/2016GL072247.

Received 13 DEC 2016
Accepted 6 FEB 2017
Accepted article online 7 FEB 2017
Published online 18 FEB 2017



# Low-frequency suppression of Southern Hemisphere tropospheric eddy heat flux

**P. Zurita-Gotor**[1,2]

[1]Universidad Complutense, Madrid, Spain, [2]Instituto de Geociencias, UCM-CSIC, Madrid, Spain

**Abstract** This paper analyzes the variability of the zonal cospectrum of Southern Hemisphere tropospheric eddy heat flux in reanalysis data. It is shown that the reduced spectral power of low-frequency eddy heat flux variability largely arises from the anticorrelation in the eddy heat transports by different zonal wave numbers. Although the most plausible mechanism for this relation invokes baroclinicity as a mediating agent, this hypothesis does not seem to be supported by the observed variability of baroclinicity. Low-frequency baroclinicity variability is primarily driven by the mean meridional circulation, with only a minor role for the eddy heat flux.

## 1. Introduction

Baroclinic instability is a key dynamical process in the extratropical atmosphere, regulating to a large extent extratropical climate. Understanding what determines the equilibrium between baroclinicity and eddy heat fluxes is a classical problem in general circulation theory, for which many conceptual models have been proposed.

A common ingredient to many of these models is the presumed sensitivity of the meridional eddy heat flux on baroclinicity, motivated by simple linear theory or more sophisticated nonlinear closures [*Held and Larichev*, 1996]. This sensitivity provides the rationale for *baroclinic adjustment* theories (see *Zurita-Gotor and Lindzen* [2007] for a review), which attribute the observed robustness of the extratropical isentropic slope to the efficient eddy transport [*Stone*, 1978]. Early modeling studies provided support for these ideas by showing that changes in transient eddy heat flux tend to compensate the reduced stationary heat transport when orography is removed in general circulation models [*Manabe and Terpstra*, 1974].

Early attempts seeking evidence of baroclinic adjustment in observed daily data had limited success. *Stone et al.* [1982] found strong correlation between baroclinicity and eddy heat flux when the heat flux leads, but no evidence of eddy heat flux sensitivity on anomalous baroclinicity. While Stone's analysis may have been marred by limited data availability, the recent study of *Thompson and Birner* [2012] using modern reanalysis data also failed to find a significant relation between Northern Hemisphere baroclinicity and eddy heat flux on monthly time scales. The authors showed that this was due to the striking compensation between synoptic and low-frequency eddy heat fluxes—only the former increase with enhanced baroclinicity. While it makes sense that planetary and synoptic eddies have opposite effects on slow baroclinicity variability, the former driving it and the latter damping it, their degree of compensation is striking and reminiscent of old baroclinic adjustment results.

On the other hand, *Thompson and Woodworth* [2014] have recently shown that Southern Hemisphere eddy heat flux variability is quasiperiodic with a characteristic time scale of 20–25 days. *Thompson and Barnes* [2014] interpret this results in terms of the *two-way* relation between eddy heat flux $h = \overline{v'\theta'}$ and baroclinicity $b = -\overline{\theta}_y$. The thermodynamic balance implies a correlation between $h$ and $\dot{b}$ (the time derivative of $b$), and Thompson and Barnes show that there exists a similar relation between $b$ and $\dot{h}$, such that heat fluxes increase on average when baroclinicity is large. While this relation is consistent with the sensitivity of the eddy heat fluxes on baroclinicity, note that such a relation is inevitable for stationary time series (the lagged covariance between $b$ and $\dot{h}$ is a lag-mirror of that between $h$ and $\dot{b}$ because their respective cross spectra are complex conjugates). In particular, one would still find a positive correlation between $b$ and $\dot{h}$ if the eddy heat flux was forced externally and baroclinicity simply responded passively. As noted by *Byrne et al.* [2016], caution is required when inferring causal relationships from lagged covariances.

This work aims to shed light on the relation between baroclinicity and eddy heat flux by analyzing the variability of the eddy heat flux zonal cospectrum in the Southern Hemisphere. We show that the eddy heat transports by different zonal waves are negatively correlated at low frequency and that it is this anticorrelation that accounts for the reduced heat flux spectral power for periods longer than 20–25 days. We investigate the implications of this result for the low-frequency variability of baroclinicity and the consistency of this variability with baroclinic adjustment.

## 2. Data and Methods

We use Southern Hemisphere (SH) data from the interim re-analysis of the European Centre for Medium-Range Weather Forecasts (ERA-Interim [*Dee et al.*, 2011]) for the period of 1 January 1979 to 31 December 2015 (13,514 days overall) at 2.5° horizontal resolution. We analyze the time series of daily-mean, zonal-mean variables and eddy fluxes (eddies are defined as deviations from the instantaneous zonal mean and denoted with primes), deseasonalized by subtracting the first four harmonics of the daily climatology. Daily-mean eddy fluxes are calculated averaging the fluxes computed at 6 h intervals.

We use standard methods of analysis. When computing empirical orthogonal functions (EOFs), the gridded data are weighted by the square root of mass prior to the computation of the covariance matrix. *Thompson and Woodworth* [2014] define the baroclinic annular mode (BAM) as the leading mode of vertically integrated eddy kinetic energy and show that this mode is highly correlated with the leading mode of eddy meridional heat flux. We focus on this latter field in our analysis of BAM-like variability. To gain a better understanding of this variability we analyze its zonal cospectrum, defined by the partition of the total flux into its zonal Fourier components. The cospectrum is computed as $\overline{v'\theta'}(k,t) = 2Re\{V(k,t)T^*(k,\ t)\}$, where $V$ and $T$ are the zonal Fourier components of $v(x,t)$ and $\theta(x,t)$, respectively.

We assess the statistical significance of correlations using $t$ tests with a reduced number of degrees of freedom to take into account the intrinsic memory. For the frequency analyses, we average 30 realizations obtained dividing the full time series into segments 870 days long (lowest resolved frequency 0.0011 days$^{-1}$), with 435 day overlapping and modulation by a Hanning window. The resulting spectra are further averaged in frequency by using a centered 5-point moving average (with two neighbors on each side), so that each spectral estimate incorporates 150 degrees of freedom. Statistical significance is assessed by using the tests of *Amos and Koopmans* [1963] for the squared coherence. Unless otherwise indicated, the cross spectra presented in this work have been normalized with the square root of the product of the power spectra, so that the real (imaginary) parts of these cross spectra can be interpreted as the in-phase (out-of-phase) correlations over the different frequency bands.

## 3. Results

Figure 1a shows the time-mean zonal cospectrum of the Southern Hemisphere tropospheric eddy heat flux, density-averaged from the surface to 300 hPa. The eddy heat flux is maximum over the midlatitude band 40 to 60°S, where it is dominated by the contributions of medium-scale waves ($k = 4$ to 6) in agreement with previous studies [*Solomon*, 1997]. The meridional average of this flux over the 40–60°S band (Figure 1b, blue line) has a peak at $k = 5$. We focus on the deseasonalized variability of this cospectrum in the present study. As might be expected, the eddy heat flux variability is strongest for the zonal waves that dominate the time-mean transport, although long-wave heat flux also tends to be more variable than short-wave heat flux (Figure 1b).

Figure 1c shows the correlation matrix between the different zonal components of the eddy heat flux. Except for the shortest waves ($k = 8$–10), the eddy heat fluxes by the different waves are negatively correlated. Although the correlations are small, ranging from 0.05 to 0.15, they are still significant at a 99% confidence level (only correlations exceeding this threshold are included in the figure). The largest negative correlation is found for waves 4 and 5 ($-0.13$). These correlations naturally increase when the waves are grouped in spectral bands. For instance, the correlation between the bands [$k = 1$–4] and [$k \geq 6$] is $-0.24$, consistent with the compensation between planetary and synoptic heat transport found by *Thompson and Birner* [2012]. More generally, Figure 1d shows how the eddy heat flux transported by any given zonal wave number is correlated with the aggregate heat flux by all other waves. The largest negative correlation is found for zonal wave

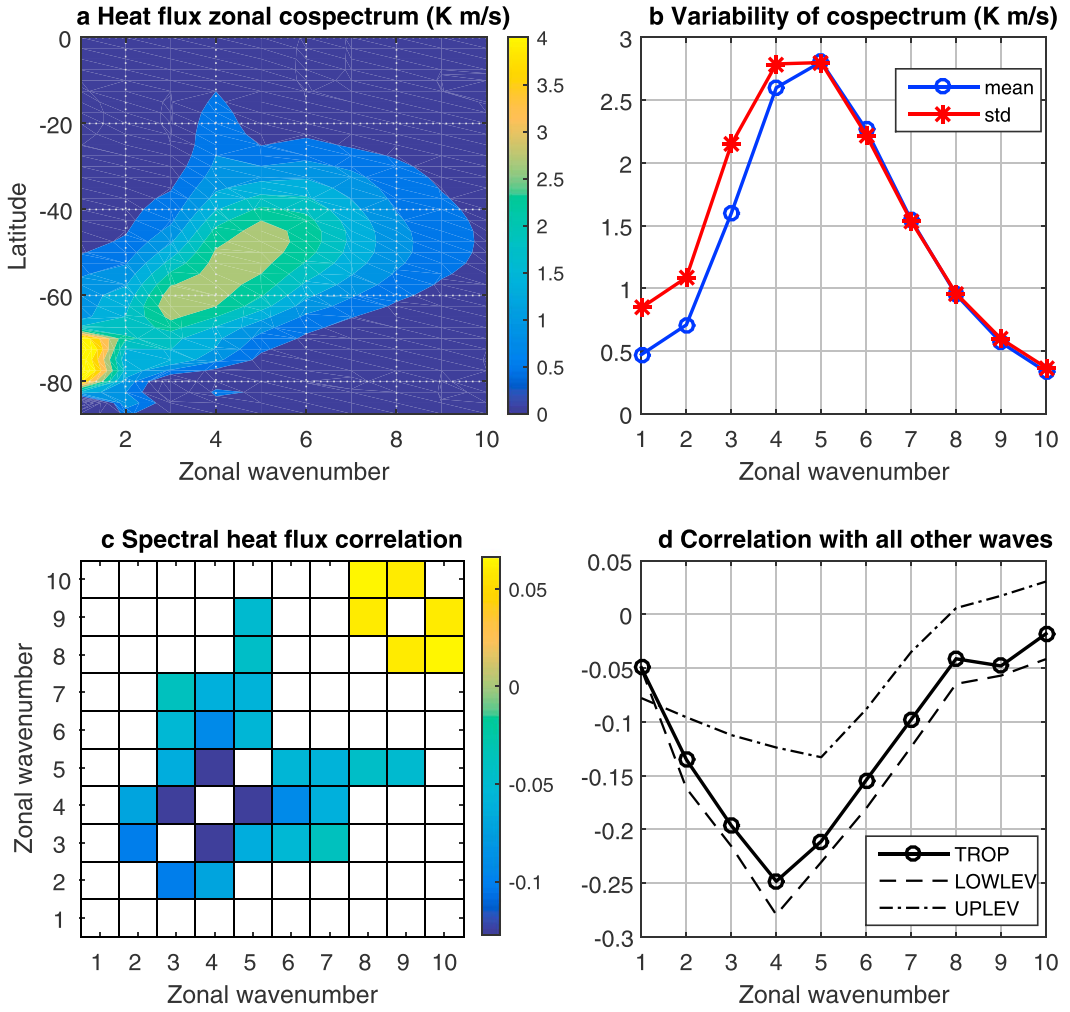


**Figure 1.** (a) Mean zonal cospectrum of the density-weighted vertical average (surface to 300 hPa) eddy heat flux, as a function of latitude. (b) Mean zonal cospectrum (surface to 300 hPa and 40 to 60°S density-weighted average) and its standard deviation. (c) Correlation matrix between eddy heat fluxes by zonal waves 1 to 10 (only values significant at a 99% level are shown). (d) Correlations between the heat flux by an individual zonal wave and the aggregate heat flux by all other waves for the vertically integrated heat flux over the full troposphere (thick solid line), the lower troposphere (700–1000 hPa, dashed), and the upper troposphere (250–400 hPa, dash-dotted).

number $k = 4$ (−0.25). Figure 1d also shows similar, aggregate correlations for the lower (700–1000 hPa) and upper (250–400 hPa) tropospheric components of the eddy heat flux (see Figures S1a and S1b in the supporting information for the full correlation matrices). It is apparent that the lower trosposphere heat flux is the dominant contributor to the observed anticorrelation, although upper troposphere correlations remain significant in many cases. Finally, Figure S1c shows the lagged structure of the autocorrelation and cross-correlation functions for the total eddy heat flux and some of its zonal components.

To assess the frequency bands responsible for the observed correlations, Figure 2 provides a spectral description of eddy heat flux variability. Figure 2a shows the power spectrum for the mass-weighted integral (40 to 60°S, surface to 300 hPa) of the tropospheric eddy heat flux (black line). The most remarkable feature is the sharp dropoff for periods longer than about 25 days, consistent with the results of *Thompson and Barnes* [2014] for BAM. However, the decay on the high-frequency side of the peak does not seem as pronounced as in their diagnostics. This difference is due to the different conventions used. As shown in Figure S1d, the high-frequency eddy heat flux power drops off more steeply in the lower than in the upper troposphere, and the 850 hPa eddy heat flux (what Thompson and Barnes show) exhibits a sharp peak. Additionally, *Wang and Nakamura* [2016] show that the peak sharpness varies with season.

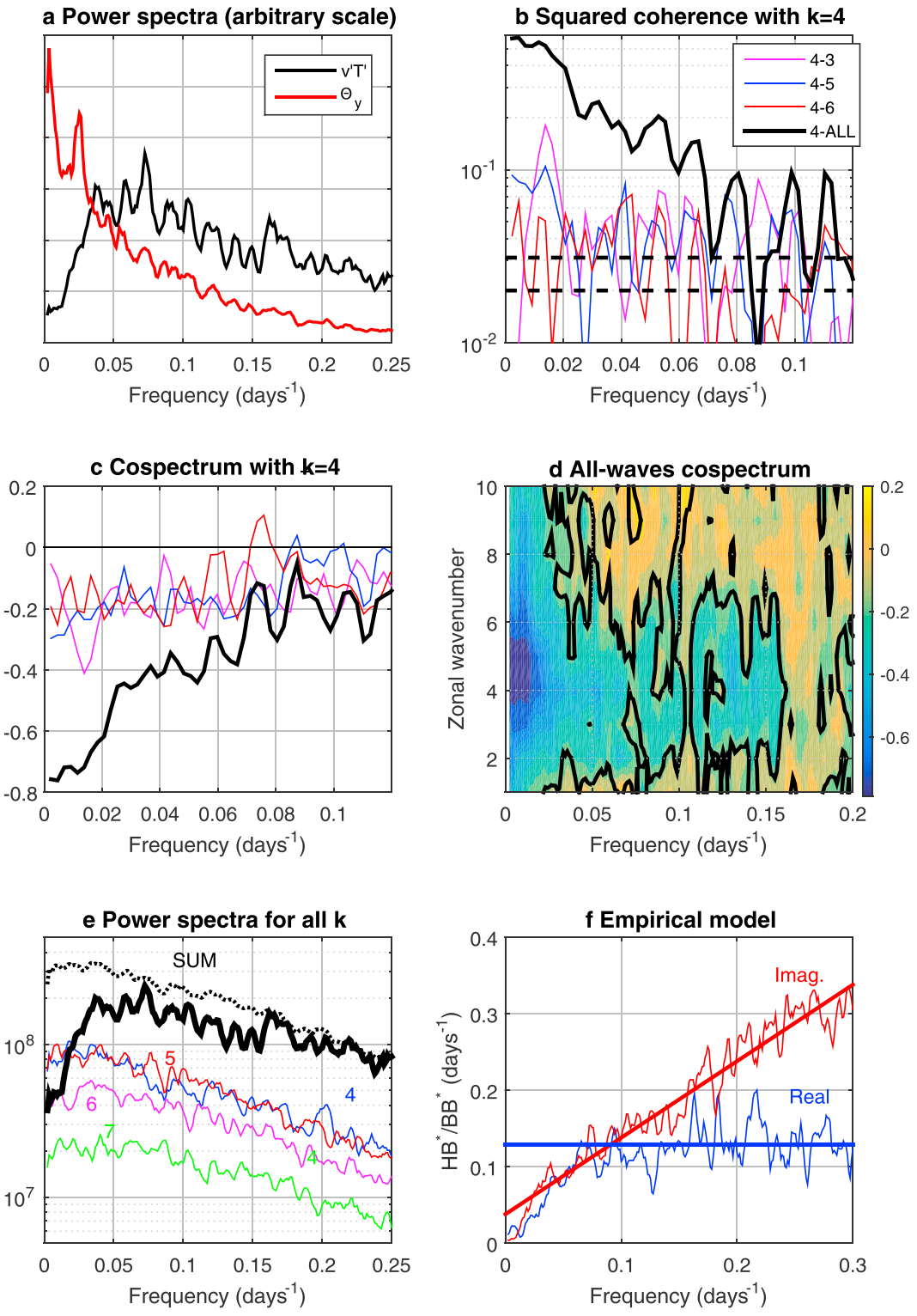


**Figure 2.** (a) Power spectra of integrated (surface to 300 hPa and 40 to 60°S) eddy heat flux and baroclinicity. (b) Squared coherence between eddy heat flux by wave $k = 4$ and heat fluxes by $k = 3$, 5, and 6 and aggregate heat flux by all waves except $k = 4$. The dashed lines show 95% and 99% confidence levels. (c) Real part of the same cross spectra. (d) Real part of the cross spectra between the heat flux by an individual wave and the aggregate heat flux by all others (the thick contour marks the 99% significance level). (e) Power spectra of heat flux by individual waves (colors), sum of heat flux power spectra for all waves (black dotted), and power spectra of net heat flux (thick black). (f) Real and imaginary parts of the normalized cross spectrum between baroclinicity and eddy heat flux, and comparison with simple model (see text for details).

Figure 2b shows the squared coherence of the cross spectra between the eddy heat transports by $k = 4$ and by other zonal waves. Consistent with the weak correlations the coherence is small, though still significant at a 99% level for the cross spectra between $k = 4$ and $k = 3$ or $k = 5$, and at the 95% level between $k = 4$ and $k = 6$. The coherence is much larger and extremely significant for the cross spectrum between the $k = 4$ heat transport and the aggregate heat transport by all other waves (black thick line). The coherence is largest at low frequency, although there are also weaker peaks over the synoptic frequency band (not visible with the displayed frequency range, see Figure S2a for a high-frequency extension of this plot). Figure 2c shows the real part of the cross spectrum over the same frequency band (the imaginary part is weak and noisy and has no obvious structure, see Figure S2b). For the individual waves, the cospectrum is unambiguously negative but small (O ($-0.2$)). The cospectrum between the $k = 4$ heat transport and the aggregate heat transport by all other waves is much more negative and reaches correlations as large as $-0.75$ at low frequency. Similar results are obtained for other zonal waves (Figure 2d, see also Figures S2c and S2d for lower/upper troposphere results)

The low-frequency anticorrelation between the different zonal components of the eddy heat flux plays a key role for the suppression of its spectral power at frequencies smaller than 0.04 days$^{-1}$. This is demonstrated in Figure 2e, which shows that the eddy heat flux spectra by individual waves (color lines) are essentially red, with some low-frequency flattening but no obvious suppression. This is consistent with the quasi-exponential decay of the autocorrelation functions for the individual heat fluxes (Figure S1c), in contrast with the oscillatory decay found for the total heat flux. The sum of the single-wave spectra (black dotted line) has the same red structure. Differences between this sum and the spectrum for the total eddy heat flux arise as a result of the correlations between its components, which lead to a drastic reduction of the net heat flux at low frequency. Figure S2e shows that about half of this reduction can be attributed to the correlations between wave number 4 and other zonal waves, most importantly zonal waves 3, 5, and 6.

Why are single-wave heat fluxes negatively correlated at low frequency? The most plausible explanation is that this relation might be mediated by baroclinicity: when baroclinicity is depleted by heat transport by a given zonal wave, other waves are less likely to transport heat. This would be consistent with the mechanism proposed by *Thompson and Barnes* [2014] for the observed quasi-oscillatory character of BAM and with classical baroclinic adjustment theory. To test this hypothesis, we next investigate the dynamics of low-frequency baroclinicity variability.

The spectrum of the meridional potential temperature gradient (averaged meridionally and vertically as the eddy heat flux) is displayed alongside the heat flux spectrum in Figure 2a (red line). The spectrum is essentially red, except for a conspicuous peak at frequencies smaller than BAM also (barely) apparent in the eddy heat flux power spectrum. This peak appears to be associated with high-latitude temperature variability and is much reduced when baroclinicity is projected on the BAM pattern instead of meridionally integrated (not shown). The redness of baroclinicity is not necessarily inconsistent with weak low-frequency heat flux forcing because time integration enhances low-frequency variability, which might mask the BAM peak.

For example, *Thompson and Barnes* [2014] use a schematic description of baroclinicity variability to illustrate their conceptual model for BAM:

$$\frac{\partial b}{\partial t} = \alpha h - \frac{b}{\tau}$$

where $b$ is baroclinicity, $h$ is eddy heat flux, $\alpha$ is a constant, and $\tau$ is a damping time scale. This relation implies that any spectral peak for $h$ will also show up in $b$, although the $b$ peak may be masked at low frequency by the response to the background (nonoscillatory) $h$ spectrum. An illustration of this low-frequency enhancement is provided by the conspicuous baroclinicity peak at ~0.025 days$^{-1}$, in response to a much weaker peak in the eddy heat flux spectrum (cf. Figure 2a).

To test the validity of this simple model, we take the Fourier transform of the above equation, which yields the following prediction for the cross spectrum between $B(\nu)$ and $H(\nu)$ (the Fourier transforms of $b$ and $h$, respectively, where $\nu$ is frequency):

$$\alpha \frac{B^* H}{B^* B} = i\nu + \frac{1}{\tau}$$

Figure 2f shows the real and imaginary parts of the normalized baroclinicity-heat flux cross spectrum by using an empirical fit for $\alpha$. For frequencies larger than about 0.1 days$^{-1}$, the cross spectrum agrees well with the predicted behavior taking $\tau \approx 7.7$ days. However, the simple model fails at low frequency, when the real part of the cross spectrum goes to zero instead of remaining constant. Note that the model's failure is independent of any assumptions made on the character of the heat flux spectrum. Rather, this failure suggests that observed low-frequency baroclinicity variability is not consistent with its being driven by *h* alone. There are two reasons why this may happen: (i) in reality, baroclinicity is not driven by the eddy heat flux but by its second derivative, and (ii) other terms neglected in the thermodynamic equation may be important. We show below that both factors play a role.

Following *Blanco-Fuentes and Zurita-Gotor* [2011], we investigate the driving of low-frequency baroclinicity variability by analyzing the relations between baroclinicity and its forcing terms in the vertically integrated thermodynamic equation (vertical integrals are denoted with angle brackets $\langle\rangle$):

$$\frac{\partial\langle\overline{\theta}_y\rangle}{\partial t} = -\frac{\partial}{a\partial\varphi}\left(\frac{1}{\cos\varphi}\frac{\partial\left\langle\overline{v'\theta'}\right\rangle\cos\varphi}{a\partial\varphi}\right) - \frac{\partial}{a\partial\varphi}\left\langle\overline{\omega}\Theta_p\right\rangle + \text{other terms}$$

The first two terms on the right-hand side represent the eddy heat flux forcing and the adiabatic heating by the mean meridional circulation (MMC), respectively. We group all other terms together with the diabatic heating and any discretization errors into a residue. *Blanco-Fuentes and Zurita-Gotor* [2011] project spatially all the above terms on the leading EOF of baroclinicity variability, which has dipolar structure and is highly correlated with SAM. Here we project instead on the baroclinicity pattern congruent with the heat flux variability, obtained regressing $\langle\overline{\theta}_y\rangle(y,t)$ on BAM. This structure, shown with a solid line in Figure 3a, is very similar to *the second mode* of baroclinicity variability (dashed, we stress again that the first baroclinicity mode is a shift) and the results described below are robust when projecting on that mode instead.

Figure 3b describes the average lifecycle of baroclinicity anomalies, computed lag-regressing the baroclinicity time series on each of its forcing terms. At short lags, baroclinicity essentially responds to the eddy heat flux forcing. In contrast, at long lags the heating by the mean meridional circulation forcing dominates and is largely balanced by the residue. These results are strikingly similar to those found by *Blanco-Fuentes and Zurita-Gotor* [2011] for baroclinicity variability along the direction of the zonal index, suggesting that the mechanistic description of baroclinicity variability presented in that paper as evidence of an eddy baroclinic feedback on the zonal index [*Robinson*, 2000] is in fact quite general and not specific to that mode.

The important role played by the low-frequency MMC forcing is further emphasized in Figure 3c, which shows that this is the dominant term for $\nu < 0.05$ days$^{-1}$. It is also striking that the power spectrum of the eddy heat flux forcing is very different from that of eddy heat flux itself (as also noted by *Wang and Nakamura* [2016]). The eddy heat flux forcing spectrum is quite white, except for a weak broad peak at periods 5 to 10 days, and is not suppressed at low frequency. (This spectrum is again strongly constrained by the low-frequency relations between the different zonal components of the eddy heat flux forcing. The forcing spectra for individual zonal waves have a red structure similar to Figure 2e (not shown).) Finally, Figure 3d shows the real part of the normalized cross spectra $B^*F_k/B^*B$ between the various forcing terms $F_k$ and baroclinicity. These must add up to zero when damping (or the residue) is included as an additional forcing term and the balance is closed. Following *Blanco-Fuentes and Zurita-Gotor* [2011], we associate positive (negative) values of the cospectra with driving (damping) of baroclinicity variability. The results are again consistent with those of the previous paper and suggestive of MMC driving at low frequency. The low-frequency eddy heat flux forcing is small due to the robust cancelation between positive and negative tendencies by planetary and synoptic waves (Figure S2f).

The fact that low-frequency baroclinicity variability cannot be reproduced by using the eddy heat flux alone may seem surprising because *Thompson and Woodworth* [2014] have reported a weak connection between eddy momentum fluxes and BAM variability (cf. their Figure 4b). We have found that the eddy momentum fluxes are in fact more connected to baroclinicity variability than to eddy heat flux variability.

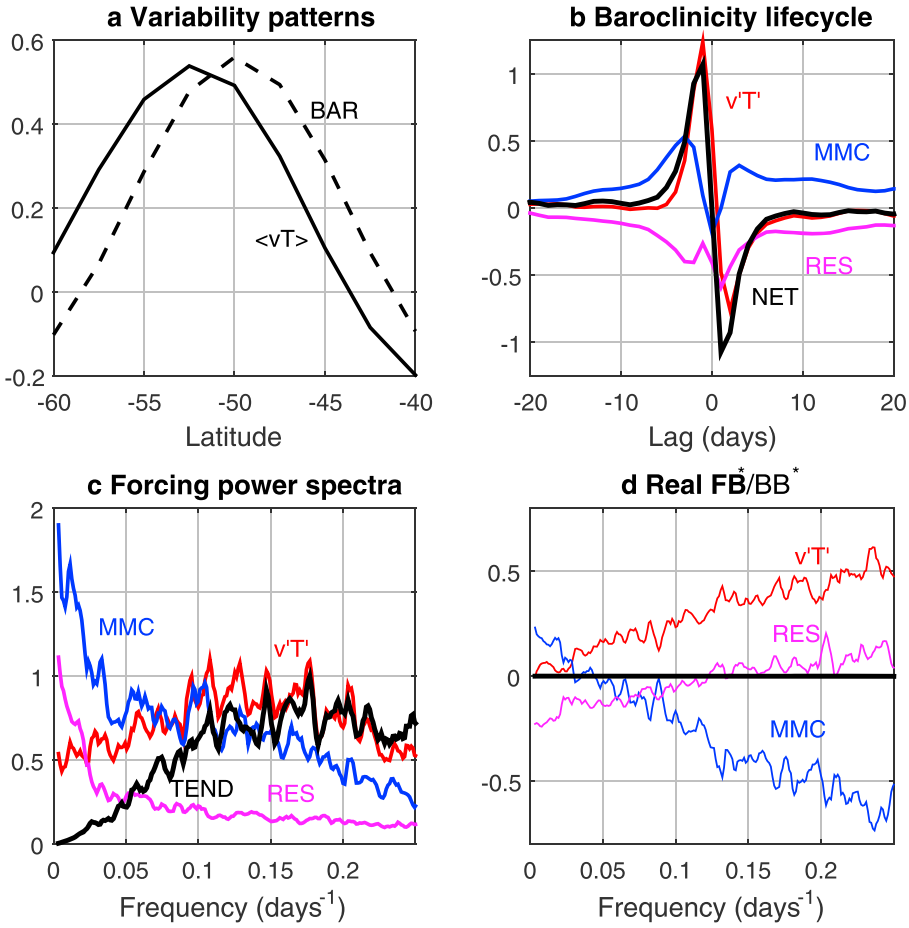


**Figure 3.** (a) Baroclinicity pattern associated with the leading EOF of vertically-integrated (surface to 300 hPa) eddy heat flux variability (solid), and second mode of baroclinicity variability (dashed). (b) Lagged correlations between baroclinicity and its main forcings, in $K^2(1000\,\mathrm{km})^{-2}\,\mathrm{d}^{-1}$. Forcings lead for negative lags, and the black line shows correlation with the net forcing/baroclinicity tendency. (c) Power spectra of the same forcings in Figure 3b. (d) Real part of the normalized cross spectra between baroclinicity and its forcings (see text for interpretation).

This is shown in Figure S3, which compares the regressions of the eddy heat and momentum flux contributions to the Eliassen-Palm divergence [*Edmon et al.*, 1980]:

$$D_z = \frac{\partial}{\partial p}\left(\frac{f}{\Theta_p}\overline{v'\theta'}\cos\varphi\right) \qquad D_y = -\frac{1}{a\cos\varphi}\frac{\partial}{\partial\varphi}\left(\overline{u'v'}\cos^2\varphi\right)$$

on the standardized principal component time series for the leading mode of eddy heat flux variability (left) and the second mode of baroclinicity variability (right). All regressions are vertically integrated over the free troposphere, from the heat flux maximum to the tropopause (800 to 250 hPa). There are significant differences between both regressions. For the eddy heat flux regressions (left) $D_y$ is in quadrature with $D_z$ consistent with the expected lead-lag regression for a baroclinic lifecycle [*Simmons and Hoskins*, 1978], and also much smaller. In contrast, $D_y$ and $D_z$ covary and add up during baroclinicity variability (right), as they must since it is their sum that drives this variability through the eddy-induced residual circulation. More interestingly, the two Eliassen-Palm components are now comparable, with the eddy momentum flux contribution dominating at long lags.

## 4. Discussion

We have presented in this work a frequency analysis of observed SH tropospheric eddy heat flux variability in ERA-interim data. Consistent with previous findings by *Thompson and Woodworth* [2014] and *Thompson and*

*Barnes* [2014], the sharp dropoff in the eddy heat flux power spectrum for periods longer than 20–25 days implies that low-frequency eddy heat flux variability is strongly suppressed. We have shown that this suppression largely results from the low-frequency anticorrelation of the heat transports by individual zonal waves, all which exhibit red variability. The anticorrelation is larger, and the spectral suppression more pronounced for the lower troposphere eddy heat flux, possibly reflecting the near-surface thermal damping [*Wang and Nakamura*, 2015]. In contrast, the power dropoff on the high-frequency side of the heat flux spectral maximum is not as sharp in our diagnostics and depends on conventions.

The low-frequency anticorrelation between different-wave heat transports is consistent with early modeling results on the compensation between stationary and transient eddy heat transport [*Manabe and Terpstra*, 1974] and with more recent observational results by *Thompson and Birner* [2012] and *Blanco-Fuentes and Zurita-Gotor* [2011]. This compensation has been traditionally explained from the perspective of baroclinic adjustment, which postulates that baroclinicity is strongly constrained by the efficiency of eddy transport [see *Zurita-Gotor and Lindzen*, 2007]. Relatedly, *Thompson and Barnes* [2014] have recently proposed that the quasiperiodic character of BAM may be due to the two-way relation between eddy heat flux and baroclinicity, and in particular to the sensitivity of eddy growth on baroclinicity. Based on these ideas, we might expect baroclinicity to act as a mediator in the eddy heat flux anticorrelation.

A difficulty with this hypothesis is that low-frequency baroclinicity variability does not appear to be constrained by the weakness of eddy heat transport. The conceptual model of baroclinicity variability of *Thompson and Barnes* [2014], which neglects other forcings, can only be made consistent with observed baroclinicity variability if the diabatic damping rate decreases at low frequency. This suggests that some other missing forcings may be driving baroclinicity variability at low frequency, a conjecture supported by our regression analysis. The analysis suggests that low-frequency baroclinicity variability is driven by adiabatic heating by the mean meridional circulation, as previously found by *Blanco-Fuentes and Zurita-Gotor* [2011] for zonal-index baroclinicity variability. A point of caution is that diabatic heating is also important and largely balances the MMC forcing. Since this term is calculated as a residue, it may incorporate discretization errors and artificial heating sources by data assimilation.

We have recently become aware of a related study by *Wang and Nakamura* [2016, in press], who also note some inconsistencies between the observed coupled eddy heat flux-baroclinicity variability and the oscillator model of *Thompson and Barnes* [2014]. Wang and Nakamura propose an alternative model for BAM based on frequency interference for modes *with the same zonal wave number*. While their model might explain the enhancement of the eddy heat flux spectrum at the BAM peak, our results suggest that the low-frequency suppression requires the compensating effects of different zonal waves.

If the low-frequency eddy heat flux suppression is not due to baroclinic feedback, what causes it? A possible explanation is that this suppression reflects a constraint on total wave activity. In the formulation of *Nakamura and Zhu* [2010], the eddy heat flux represents a wave activity source, but part of this wave-mean flow interaction is reversible because eddy dissipation is limited by the small effective diffusivity. At low frequency, when transience is weak, the wave activity source must be limited by the strength of dissipation [*Zurita-Gotor et al.*, 2014]. This might explain why only the eddy heat flux—and not the actual eddy baroclinicity forcing (its second meridional derivative)—is suppressed at low frequency, since it is really the former that drives wave activity variability. *Wang and Nakamura* [2015, 2016] show evidence of quasiperiodic variability in wave activity diagnostics during austral summer. An alternative explanation suggested by a reviewer is that a single zonal wave number dominates the heat transport at any given time, with the dominant wave vacillating across different wave numbers through nonlinear interactions. We are currently investigating these questions by using idealized simulations with a quasi-geostrophic two-layer model. The eddy heat flux in this model is also suppressed at low frequency, although the high-frequency spectrum is far less peaked than in observations, which we attribute to weak model damping and large wave activity transience.

**Acknowledgments**

We are grateful to the Editor and to two anonymous reviewers for their thoughtful comments and for helpful suggestions that improved the manuscript. We thank the European Centre for Medium-Range Weather Forecasts for making the reanalysis data available. The data used in this study can be downloaded from http://www.ecmwf.int/, and the scripts used to process these data are available upon request.

## References

Amos, D. E., and L. H. Koopmans (1963), *Tables of the Distribution of the Coefficient of Coherence for Stationary Bivariate Gaussian Processes (No. SCR-483)*, Sandia Corp., Albuquerque, N. M.

Blanco-Fuentes, J., and P. Zurita-Gotor (2011), The driving of baroclinic anomalies at different timescales, *Geophys. Res. Lett.*, *38*, L23805, doi:10.1029/2011GL049785.

Byrne, N. J., T. G. Shepherd, T. Woollings, and R. A. Plumb (2016), Annular modes and apparent eddy feedbacks in the Southern Hemisphere, *Geophys. Res. Lett.*, *43*, 3897–3902, doi:10.1002/2016GL068851.

Dee, D. P., et al. (2011), The ERA-Interim reanalysis: Configuration and performance of the data assimilation system, *Q. J. R. Meteorol. Soc.*, *137*(656), 553–597.

Edmon, H. J., B. J. Hoskins, and M. E. McIntyre (1980), Eliassen-Palm cross sections for the troposphere, *J. Atmos. Sci.*, *37*(12), 2600–2616.

Held, I. M., and V. D. Larichev (1996), A scaling theory for horizontally homogeneous, baroclinically unstable flow on a beta-plane, *J. Atmos. Sci.*, *53*(7), 946–952.

Manabe, S., and T. B. Terpstra (1974), The effects of mountains on the general circulation of the atmosphere as identified by numerical experiments, *J. Atmos. Sci.*, *31*(1), 3–42.

Nakamura, N., and D. Zhu (2010), Finite-amplitude wave activity and diffusive flux of potential vorticity in eddy-mean flow interaction, *J. Atmos. Sci.*, *67*(9), 2701–2716.

Robinson, W. A. (2000), A baroclinic mechanism for the eddy feedback on the zonal index, *J. Atmos. Sci.*, *57*(3), 415–422.

Simmons, A. J., and B. J. Hoskins (1978), The life cycles of some nonlinear baroclinic waves, *J. Atmos. Sci.*, *35*(3), 414–432.

Solomon, A. B. (1997), An observational study of the spatial and temporal scales of transient eddy sensible heat fluxes, *J. Clim.*, *10*(3), 508–520.

Stone, P. H. (1978), Baroclinic adjustment, *J. Atmos. Sci.*, *35*(4), 561–571.

Stone, P. H., S. J. Ghan, D. Spiegel, and S. Rambaldi (1982), Short-term fluctuations in the eddy heat flux and baroclinic stability of the atmosphere, *J. Atmos. Sci.*, *39*, 1734–1746, doi:10.1175/1520-0469(1982)039<1734:STFITE>2.0.CO;2.

Thompson, D. W., and E. A. Barnes (2014), Periodic variability in the large-scale Southern Hemisphere atmospheric circulation, *Science*, *343*(6171), 641–645.

Thompson, D. W., and J. D. Woodworth (2014), Barotropic and baroclinic annular variability in the Southern Hemisphere, *J. Atmos. Sci.*, *71*(4), 1480–1493.

Thompson, D. W., and T. Birner (2012), On the linkages between the tropospheric isentropic slope and eddy fluxes of heat during Northern Hemisphere winter, *J. Atmos. Sci.*, *69*(6), 1811–1823.

Wang, L., and N. Nakamura (2015), Covariation of finite-amplitude wave activity and the zonal mean flow in the midlatitude troposphere. Part 1: Theory and application to the Southern Hemisphere summer, *Geophys. Res. Lett.*, *42*, 8192–8200, doi:10.1002/2015GL065830.

Wang, L., and N. Nakamura (2016), Covariation of finite-amplitude wave activity and the zonal mean flow in the mid-latitude troposphere. Part 2: Eddy forcing spectra and the periodic behavior in the Southern Hemisphere summer, *J. Atmos. Sci.*, doi:10.1175/JAS-D-16-0091.1, in press.

Zurita-Gotor, P., and R. S. Lindzen (2007), Theories of baroclinic adjustment and eddy equilibration, in *The Global Circulation of the Atmosphere*, edited by T. Schneider and A. Sobel, pp. 22–46, Princeton Univ. Press, Princeton, N. J.

Zurita-Gotor, P., J. Blanco-Fuentes, and E. P. Gerber (2014), The impact of baroclinic eddy feedback on the persistence of jet variability in the two-layer model, *J. Atmos. Sci.*, *71*(1), 410–429.